MAHASAGAR
Vol.26, No.2 (December), 1993, pp. 95-104.

OBSERVED CURRENTS AT BOMBAY HIGH DURING A WINTER

A.A. FERNANDES, P. CHANDRAMOHAN AND B.U. NAYAK
National Institute of Oceanography,
Dona Paula, Goa - 403 004

ABSTRACT

Ten day records of Aanderaa current meters (24 Dec 1981 to 2 Jan 1982) at four depths, *viz.* 30, 45, 60 and 75 m at Bombay High (19° 24.5'N, 71° 2.5'E) off the west coast of India, in a water depth of 80 m have been subjected to spectral, cross-spectral, rotary spectral, harmonic analysis, and low pass filtering in the frequency domain.

It was found that at semidiurnal and diurnal frequencies the currents were predominantly barotropic. At all depths the tidal ellipses corresponding to the semidiurnal and diurnal tides were oriented roughly perpendicular to the shelf-break while the mean currents were northwestwards along the shelf-break. During the observation period, the mixed layer (~50 m) remained isothermal while a steady rise in temperature (~2° C) with time was noticed in the cooler bottom layer.

Key-words : Currents, spectra, harmonics, Bombay high.

INTRODUCTION

Bombay High is the name given to the portion of the Fifty Fathom Flat on the continental shelf off Bombay on the west coast of India. The Bombay High region owes its importance to the presence of a number of offshore oil drilling platforms, which have been connected by submarine pipelines to onshore oil refineries and an LPG bottling plant. The Bombay High is therefore a pollution hot spot.

During winter (November to February) a poleward surface current is present along the west coast of India (Cutler and Swallow, 1984). The current carrying warmer and relatively fresher water moves against the prevailing northeast monsoon winds. This current has been inferred by Shetye, Gouveia, Shenoi, Michael, Sunder, Almeida and Santanam (1991) from hydrographic data. The only instance of direct measurement of the winter current is by Varma and Gopinathan (1976).

Our measurements made at Bombay High, though short, are utilized to describe the nature and scales of variability in currents and temperature characteristics. Tidal ellipses derived from the harmonic analysis of these records can be used to calibrate numerical models for barotropic tidal circulation (see Gouveia, Backhaus and Shetye).

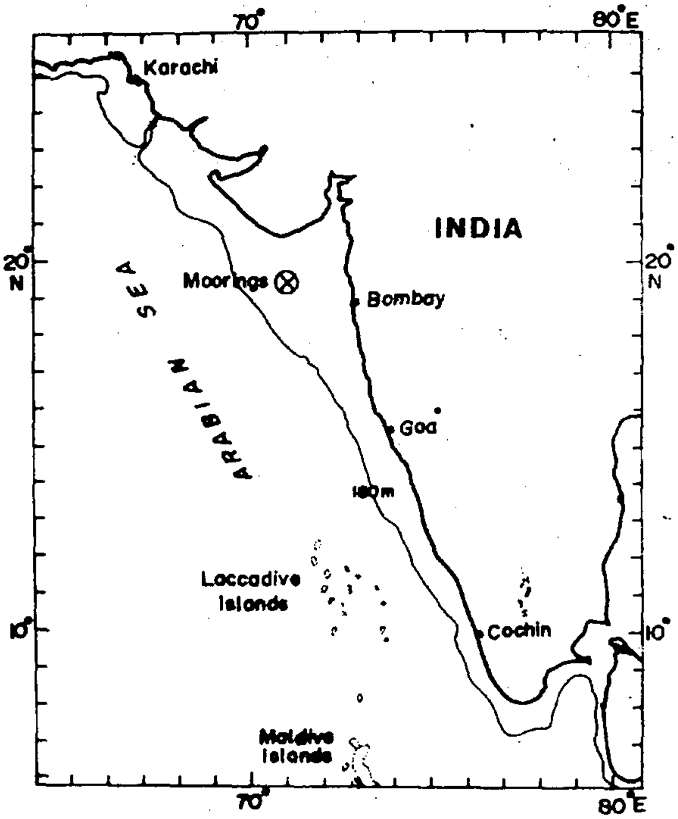

Fig. 1. Map showing location of moorings of Aanderaa current meters.

DATA AND METHODOLOGY

Two U-type moorings of current meters (Aanderaa RCM 4) were installed at Bombay High. Mooring 1 was deployed for 11 days from 23 Dec 1981 at (19°24.5′N, 71°02.5′E) in water depth of 80 m and had 4 current meters at 30, 45, 60 and 75 m depth (Fig. 1). Mooring 2 was deployed for 5 days from 28 Dec 1981 at (19° 23.7′N, 71°02.1′E) approximately 0.9 nautical miles from Mooring 1 and had current meters at 10 and 20 m depth. The sampling interval was 10 and 5 minutes for the current meters at Moorings 1 and 2 respectively. The tidal elevation was reckoned from the pressure sensor of the current meter at 30 m depth. The resolution of the tidal measurement was 7.6 cm.

The speed and direction records of these 6 current meters were first resolved to *u*- and *v*-components and these data at Mooring 1 were subjected to auto-spectral, cross-spectral and harmonic analyses.

ANALYSES

Spectra

Fig. 2 shows the rotary spectra of currents at 30 m depth computed following Gonella (1972). Two ensembles of 5 days each were used. A Hanning window in the time domain was employed. FFT algorithms that can handle time series of length N expressible as the product

$$N = 2^i . 3^j . 5^k$$

where *i*, *j* and *k* are non-negative integers, which are appropriate for handling geophysical time series were used. Rotary spectral densities were enhanced by a factor of 1/0.375 to make allowance for loss of energy due to windowing. In the spectra prominent peaks at diurnal and semidiurnal frequencies are noticed. The peak at the quarterdiurnal tide appears to be part of the noise continuum. Rotary spectra at the four levels of Mooring 1 showed that the diurnal and semidiurnal ellipses were stable at 0.05 significance level. The sense of rotation of the ellipses was clockwise. The orientation of the major axis of the ellipses was about 25° to North of east axis (Fig 3)

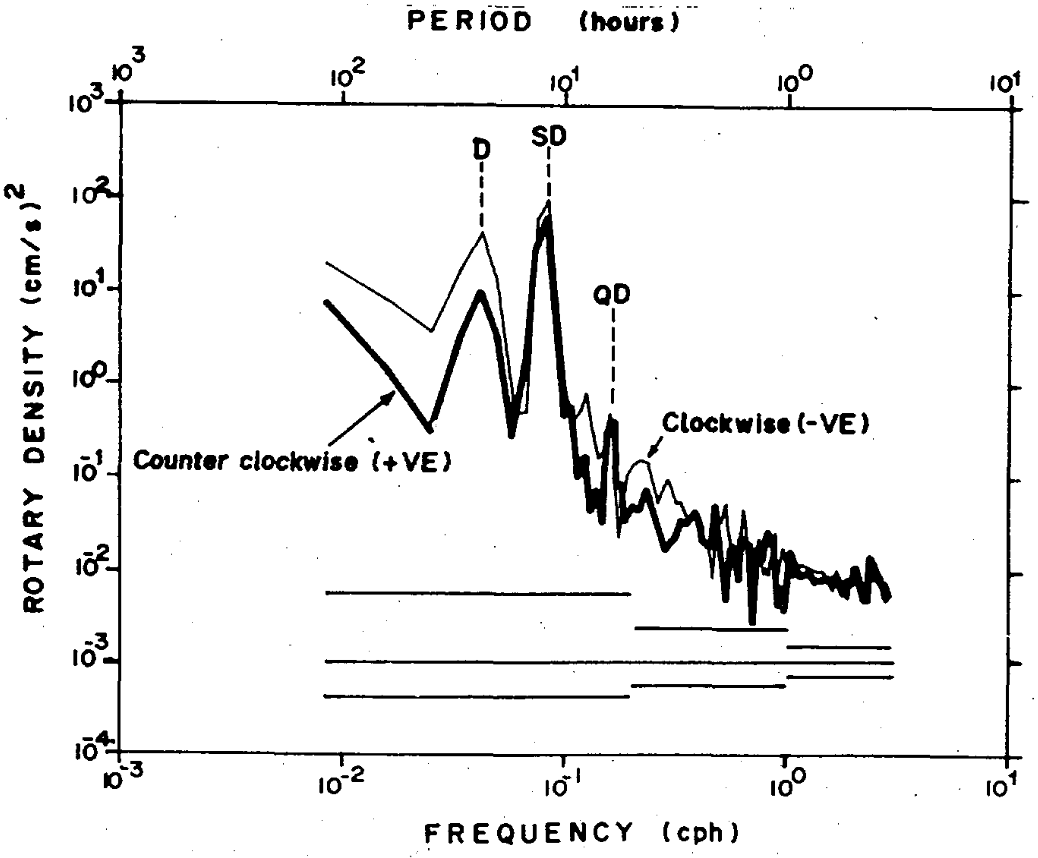

Fig. 2. Rotary spectra of currents at 30 m depth. Ninety percent confidence limits are shown.

suggesting that the tidal currents are nearly perpendicular to the shelf-break. Shenoi and Antony (1991) observed dominant inertial frequency (48 hrs period) motions off Mormugao, about 600 km to the south of Bombay during November 1986. However, the signature of inertial motions with period of about 36 hours was absent in the Bombay High data.

Table I presents the cross-spectra between the tidal elevation at the site of the moorings and the *u*-, *v*-components of the currents at 30, 45, 60 and 75 m depths. At

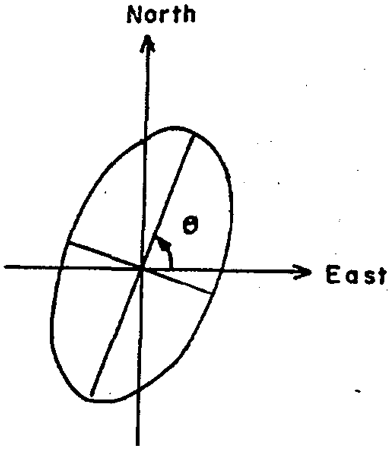

Fig. 3. Ellipse orientation θ, $-\pi/2 \le \theta \le \pi/2$. Positive value of θ indicates major axis is oriented to the North of the positive x-axis (East).

Table I – Cross-spectra between the tidal elevation at the site and current components (Mooring 1).

Depth (m)	Period (hrs)	Tide vs *u*- comp			Tide vs *v*- comp		
		Res[$]	Coh[*]	Phase[#]	Res[$]	Coh[*]	Phase[$]
30	24	1.03	0.81	058	0.77	0.85	098
	12	2.49	0.96	036	0.95	0.89	050
	6	0.47	(0.01)	173	1.00	0.84	178
45	24	1.10	0.81	054	0.81	0.79	104
	12	2.25	0.96	036	1.00	0.93	052
	6	0.66	0.77	104	1.04	(0.72)	157
60	24	1.14	0.87	054	0.91	0.91	111
	12	2.08	0.96	035	1.07	0.97	049
	6	0.76	(0.02)	119	0.54	(0.39)	160
75	24	0.92	0.80	085	0.52	0.96	123
	12	2.25	0.97	043	0.87	0.98	050
	6	0.71	(0.36)	-161	0.59	(0.40)	147

[*] Coherence below 0.73 is not significant at 0.05 significance level

[#] Positive phase difference indicates current leads the tide.

[$] Response function is the ratio of spectral density of current component to the tidal elevation.

the diurnal and semidiurnal frequencies, the tide is coherent with the currents, and the currents lead the tide. It is also evident that the semidiurnal currents at all depths are of the same phase. The diurnal currents at 30, 45 and 60 m depths are of the same phase while the currents at 75 m depth (*i.e.* 5 m above the bottom) lead the currents at shallower depths by about two hours. The phase lead at the bottom is consistent with the effects of bottom friction (Prandle, 1982). The response function in Table I gives the ratio of the spectral density of the current component to the spectral density of the tidal elevation. A comparison of the response functions shows that the energy at diurnal and semi diurnal frequencies is more or less the same at all depths for the *u*- as well as *v*-components, that the *u*-components are more energetic than the *v*-components, and that the semi-diurnal currents are twice as energetic as the diurnal currents. Since the phases, spectral density, ellipse orientation and sense of rotation at all depths except close to the bottom are about the same, the currents at diurnal and semi-diurnal frequencies may be viewed as barotropic.

Harmonic analysis

Table II presents the results of harmonic analysis and the inferred ellipse characteristics for the currents at 30, 45, 60 and 75 m depths. The original series, with 10 min sampling interval were low-pass filtered and thus converted into hourly series

Table II – Harmonic analysis of currents at Bombay High (Mooring 1).

Depth (m)	Constituent	*u*-comp		*v*-comp		Ori$^{\$}$	Semi major*	Semi minor*
		H*	g#	H*	g#			
30	M_2	19.8	317	6.8	298	18	20.8	-2.0
	S_2	8.9	004	3.9	355	24	9.7	-0.5
	K_1	6.6	350	4.4	309	31	7.5	-2.5
	O_1	3.1	320	2.4	270	33	3.6	-1.6
45	M_2	17.9	316	7.1	303	21	19.2	-1.6
	S_2	7.6	002	4.3	349	29	8.7	-0.8
	K_1	6.9	349	5.4	308	36	8.3	-3.0
	O_1	2.7	340	1.1	260	05	2.8	-1.1
60	M_2	16.8	318	7.9	300	24	18.4	-2.2
	S_2	7.5	005	4.3	351	29	8.6	-0.9
	K_1	6.7	350	5.2	292	32	7.5	-3.9
	O_1	4.2	335	3.1	286	33	4.8	-2.0
75	M_2	17.6	311	7.1	299	22	19.0	-1.5
	S_2	8.3	347	2.7	360	18	8.7	0.6
	K_1	6.3	315	2.7	274	19	6.6	-1.7
	O_1	2.3	327	1.9	246	21	2.4	-1.9

* Amplitude of constituent and length of axes (cm s^{-1})

\# Greenwich phase of constituent (deg)

\$ Ellipse orientation in degrees to N of east axis.

and were then subjected to harmonic analysis. The filter characteristics of the frequency domain filter are: unit response for periods > 6 hrs, zero response for periods < 5 hrs and linearly decreasing (frequency) response from 1 to 0 for frequencies from $1/6$ to $1/5$ cph respectively. More details about low-pass filter are given in the Section on low frequency variation. Harmonic analysis was performed by using the least squares method. An excellent treatment of the general methodology is given by Zetler, Schuldt, Whipple and Hicks (1965). Since the records were only for 10 days, the amplitudes and Greenwich phases of 4 major constituents, *viz.* M_2, S_2, K_1 and O_1 were computed.

The amplitude and phase for these constituents were corrected for the effect of neighbouring unresolvable constituents by using trigonometrical formulae similar to those derived by Dronkers (1964). The constituents M_2, S_2, K_1 and O_1 were corrected for the effect of (N_2, L_2, ν_2), (K_2, T_2), (P_1, J_1) and (Q_1, ρ_1) respectively in conformance with the semi-graphic method of Suthons (1959). The respective *u*-, *v*-components of the semi-diurnal constituents M_2 and S_2 have the same Greenwich phase at all depths; and the diurnal constituents K_1 and O_1 have the same phase at 30, 45 and 60 m depths. The phase structure as well as ellipse orientation, and lengths of semi-major and semi-minor axes of ellipses are consistent with the results of cross spectral and rotary spectral analysis.

The lengths of the semi-major and semi-minor axes show that while the M_2 and S_2 ellipses are nearly one-dimensional, the K_1 and O_1 ellipses are smaller and nearly

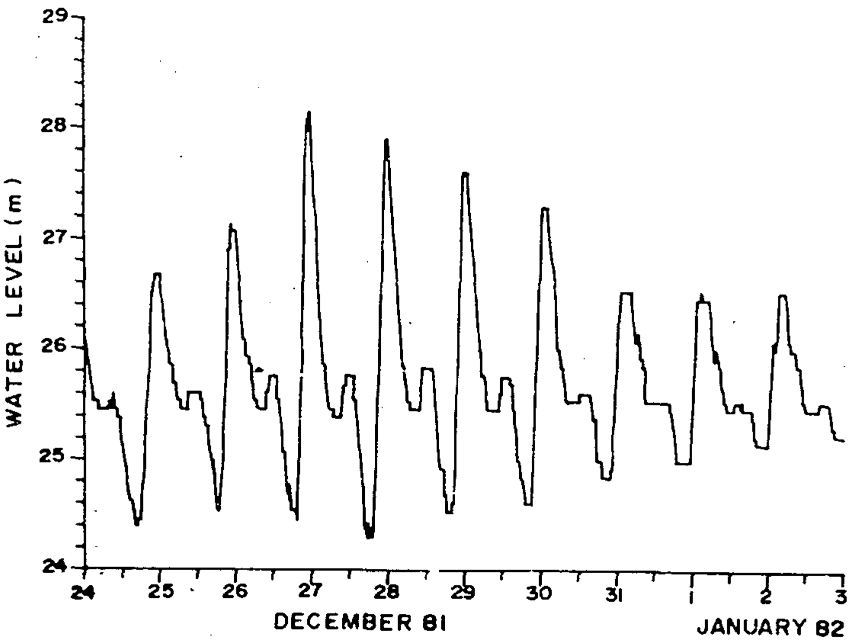

Fig. 4. Tidal elevation at mooring site reckoned from the pressure sensor of the Aanderaa current meter at 30 m depth.

circular. We notice that except for the S_2 ellipse at 75 m depth, for which the sense of rotation is anticlockwise, the sense of rotation is clockwise for all other ellipses.

Fig. 4 shows the tidal elevation at the mooring site. The coarse resolution in tidal measurement is responsible for the step-like nature of the tidal curve in the figure. The tide is characterized by a marked diurnal inequality. Besides the coarse resolution, the tidal measurements were also affected by the 'wandering' of the current meter mooring. However, Table III shows that the results of the harmonic analysis are generally consistent with the numerical computation of global tides by Schwiderski (1979,1981a,b,c). The ratio of the amplitudes ($K_1 + O_1$) : ($M_2 + S_2$) is 0.86, while the ratio ($K_1 + O_1$) : M_2 is 1.28. Both ratios indicate that the tide at Bombay High is of the mixed type.

Table III – Tidal constants at Bombay High.

Constituent	H (cm)			g(deg)		
	Obs[*]	M-20[#]	m-19[$]	Obs[*]	M-20[#]	m-19[$]
M_2	58.6	71	72	356	340	326
S_2	29.0	22	27	008	029	365
K_1	39.3	36	36	042	069	058
O_1	36.0	19	18	357	065	054

[*] Constants derived from observations at 19° 25.5′N, 71° 2.5′E
[#] Constants derived from Schwiderski's model at 20°N, 71°E
[$] Constants derived from Schwiderski's model at 19°N, 71°E.

Low frequency motions

To evaluate the low-frequency motions, a low-pass frequency domain filter was used. Frequency domain filters have an advantage over time domain filters in that one can construct a filter with any desired frequency response function. We specified unit response for periods > 48 hrs and zero response for periods < 48 hrs, so as to eliminate inertial motions and astronomical tides.

This was done by first subjecting the complete data, in one ensemble, to FFT using a box-car window. The Fourier transforms corresponding to the different periods from ∞ to the Nyquist were multiplied by 1 or 0 depending on whether the corresponding period was > 48 hrs or not. The inverse transforms were then computed to obtain the low frequency variation.

The low-frequency variations at different depths (Fig. 5) appear to be more or less in phase with one another. There is an episode from 30.12.81 to 31.12.81 when southerly currents are present at 30, 45, 60 and 75 m depths. The southerly flow continued at the 75 m depth till the end of the observation. We note that the mean currents at all the depths are northwestwards along the shelf-break. The speed and

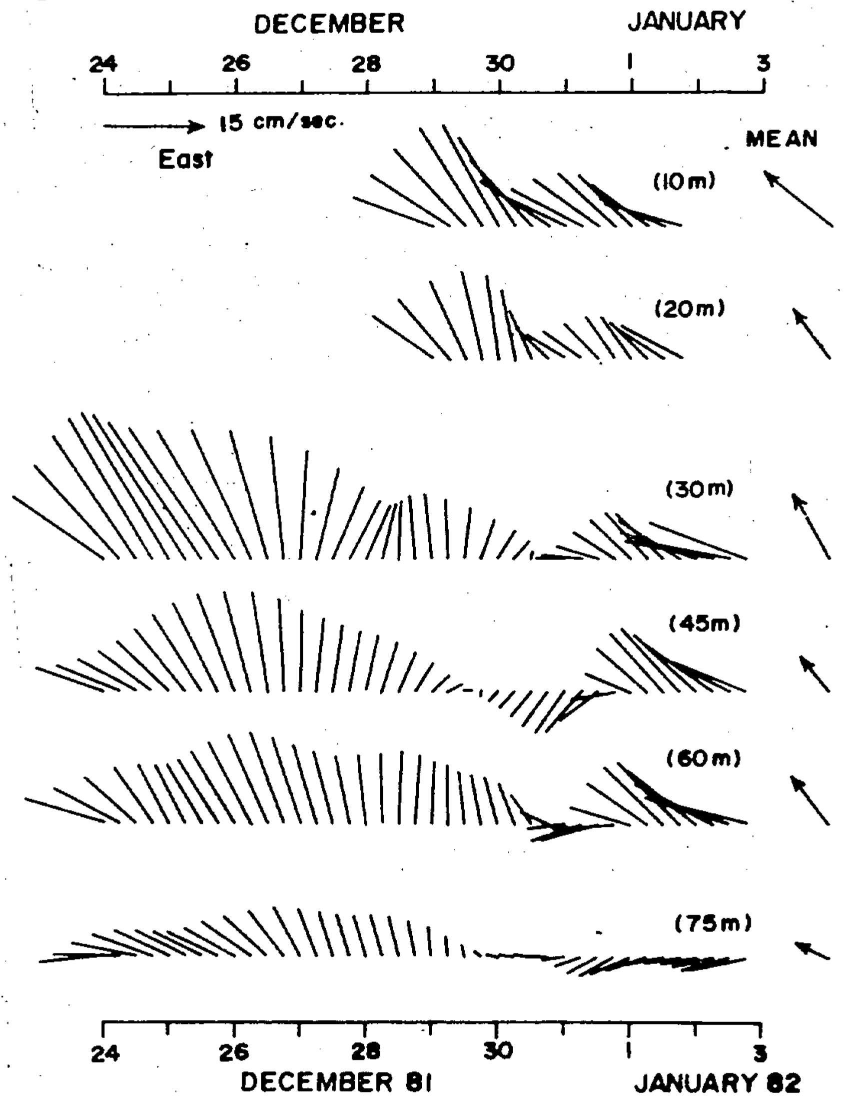

Fig. 5. Low-frequency variation (periods > 48 hrs) of currents at different depths, with time.

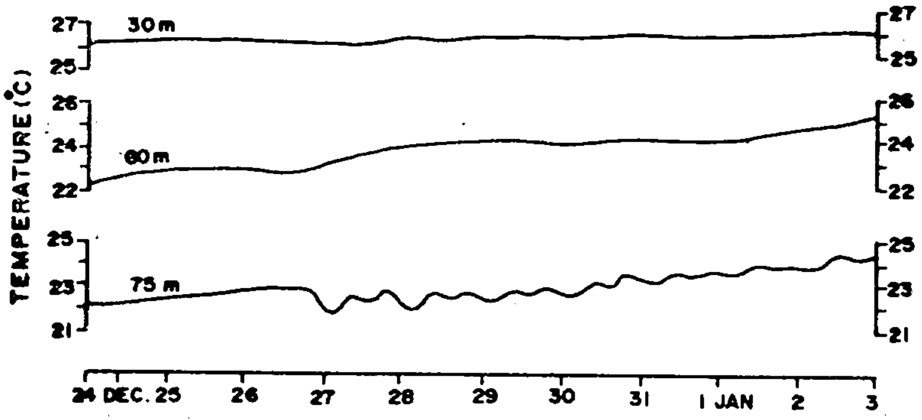

Fig. 6. Temperature variation with time at 30, 60 and 75 m depths.

direction of the mean current at 10 m depth are consistent with climatological surface currents for December and January (Cutler and Swallow, 1984).

Temperature

Throughout the record, at 10, 20, 30 and 45 m depths the temperature remained isothermal at 26.2 ± 0.1°C. At 60 m depth the temperature increased from 22.4°C at the beginning of the record to 25.3°C at the end of the record, while at 75 m depth the temperature rose from 22.1° to 24.4°C (Fig. 6). An explanation of this (~2°C) rise in temperature with time in the cooler bottom layer would be presented elsewhere.

REFERENCES

Cutler, A.N. and J.C. Swallow, 1984. Surface currents of the Indian Ocean. *IOS Report No. 187*. 88pp.

Dronkers, J.J., 1964. *Tidal Computations in Rivers and Coastal Waters*. North Holland Pub. Co., Amsterdam, 518 pp.

Gonella, J., 1972. A rotary component method for analysing meteorological and oceanographic vector time series. *Deep Sea Resarch*, **19**: 833-846.

Gouveia, A.D., J.O. Backhaus and S.R. Shetye, *. A model for Barotropic tidal currents on the eastern continental shelf of the Arabian Sea. (Unpublished)

Prandle, D., 1982. The vertical structure of tidal currents and other oscillatory flows. *Continental Shelf Research*, **1**: 191-207.

Schwiderski, E.W., 1979. Global ocean tides, Part II: The semidiurnal principal lunar tide (M_2). Atlas of tidal charts and maps. *Naval Surface Weapons Centre*. NSWC TR 79-414.

Schwiderski, E.W., 1981a. Global ocean tides, Part III: The semidiurnal principal lunar tide (M_2). *Atlas of Tidal Charts and Maps*, Naval Surface Weapons Centre, NSWC TR 81-122.

Schwiderski, E.W., 1981b. Global ocean tides, Part IV: The diurnal principal lunar tide (M_2). *Atlas of Tidal Charts and Maps*, Naval Surface Weapons Centre, NSWC TR 81-142.

Schwiderski, E.W., 1981c. Global ocean tides, Part V: The diurnal principal lunar tide (M_2). *Atlas of Tidal Charts and Maps*, Naval Surface Weapons Centre, NSWC TR 81-144.

Shenoi, S.C., M.K. Antony and D. Sundar, 1988. Nature of the observed oscillatory flows in the shelf waters of the western continental shelf of India. *Journal of Coastal Research*, **4**: 617- 626.

Shenoi, S.S.C. and M.K. Antony, 1991. Current measurements over the western continental shelf of India. *Continental Shelf Research*, **11**: 81-93.

Shetye, S.R., A.D. Gouveia, S.S.C. Shenoi, G.S. Michael, D. Sunder, A.M. Almeida and K. Santanam, 1991. The coastal current off western India during the north-east monsoon. *Deep-Sea Research*, 38: 1517-1529.

Suthons, C. T., 1959. Harmonic tidal analysis for short period observations. *Admiralty Tidal Handbook No. 3*, N.P. 122(3), Hydrographic Department, Admiralty.

Varma, K. K. and C. K. Gopinathan, 1977. Currents off Bombay during February 1976. *Mahasagar - Bulletin of the National Institute of Oceanography*, **10**: 1-8.

Zetler, B. D., M. D. Schuldt, R. W. Whipple and S. D. Hicks, 1965. Harmonic analysis of tides from data randomly spaced in time. *Journal of Geophysical Research*, **70**: 2805-2811.